06 Apr 1995, 10:30 am - 12:30 pm

Shaking Table Tests on Transient Flow of Liquefied Ground

I. Towhata
University of Tokyo, Japan

H. Toyota
University of Tokyo, Japan

Proceedings: Third International Conference on Recent Advances in Geotechnical Earthquake Engineering and Soil Dynamics, April 2-7, 1995, Volume I, St. Louis, Missouri

Shaking Table Tests on Transient Flow of Liquefied Ground

Paper No. 3.21

I. Towhata
Professor of Civil Engineering, University of Tokyo, Tokyo, Japan

H. Toyota
Department of Civil Engineering, University of Tokyo, Tokyo, Japan

SYNOPSIS: An attempt was made to predict the time history of the lateral displacement of ground that liquefied due to earthquakes. The study was initiated by model tests to examine the nature of liquefied sand. The knowledge thus obtained was combined with the theory of Lagrangean equation of motion in order to develop a method of prediction. Comparison was then made between prediction and observation.

INTRODUCTION

The purpose of this study is shaking table tests on lateral movement of liquefied ground and its application to a mathematical prediction of the amount of ground movement. The authors have been carrying out shaking tests under 1-g field on sandy deposits of relative density around 40% (Sasaki et al., 1992). One of the findings obtained in those tests was that the movement of liquefied ground terminated as soon as the input shaking was switched off.

The in-situ experiences during past earthquakes, in contrast, appear to be against this. The piers of Showa Bridge in Niigata were distorted by the lateral movement of surrounding sandy soils. An eyewitness was quoted to say (Horii, 1968) that the bridge started to fall down after the major shaking. The body of the Lower San Fernando Dam during the 1971 San Fernando earthquake is considered to have moved after the strong motion of the earthquake that induced liquefaction.

The difference of the time of ground motion between small 1-g model tests and prototypes is not totally attributed to the level of stress. Recent centrifugal shaking tests (Taboada and Dobry, 1993) on loose model slope of relative density around 40% developed lateral ground movement only during the shaking. Thus, there is a need to conduct more realistic model tests on loose sand that flows under static gravity.

Flow failure of sand is reproduced in models by considering the stress-stain behavior of sand more carefully. Fig.1 compares undrained triaxial compression tests on loose Toyoura sand. When a specimen of void ratio=0.908 was consolidated under 1960kPa, the following shear procedure revealed a strain-softening behavior after a peak shear stress. This softening suggests that an unlimited deformation or flow failure of sand is possible when the working static stress is greater than the residual strength.

A specimen of the same void ratio was consolidated under a reduced pressure of 98kPa. This specimen did not exhibit strain softening during undrained shear (Fig.1). Hence, no flow failure is likely in this material. When the void ratio was increased to 0.949 in Fig.1, a strain softening occurred again under the reduced consolidation pressure of 98 kPa. In this respect, the present study ran shaking table tests under 1-g field on very loose deposits. The low density was required in order to produce strain softening and flow failure.

TESTING METHOD

A loose deposit of Toyoura sand, as loose as 1.03 in void ratio, was prepared by a method of "wet tamping." Wet sand with water content of 5% was placed by layers in a container that was filled with CO_2 gas. The surface of each layer was lightly compacted, if necessary, to achieve the desired sand density. Then, water flew into the container slowly from the bottom so that a water-saturated ground was obtained.

Fig.2 illustrates a model ground. The length is 2m and the surface slope is either 10% or 20%. Ground displacement was studied by a grid of colored sand that was placed in the

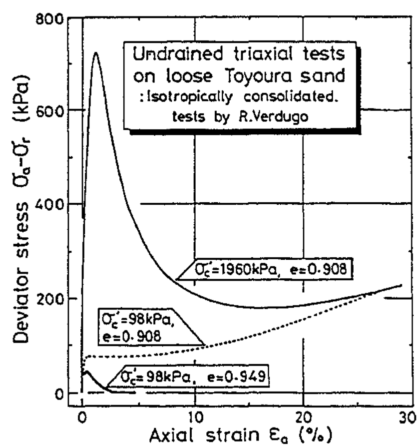

Fig.1 Undrained triaxial tests of loose sand (Verdugo, 1992).

vertical cross section. This grid indicated the overall deformation of ground after flow. Further, a displacement transducer together with accelerometers and piezometers were used.

The base shaking took place in one of the two directions. The one parallel to the slope is a conventional one, that exerts an inertia force in the direction of slope. Since the model ground was found to move in the direction of slope after liquefaction, the ground movement might be affected by the inertia force. To avoid this problem, another type of shaking, in the direction perpendicular to slope, was employed as well. This perpendicular was of impulse type, which continued for a very short period after which the base motion diminished. Since the sand was very loose, this short shaking was able to trigger an overall liquefaction. The flow of model ground occurred under a static gravity field as desired.

TESTS WITH IMPULSE SHAKING

Fig.3 indicates a test in which a model ground of e=1.03 was shaken perpendicular to slope by impulse. See the very short duration of base excitation. Excess pore water pressure immediately reached the initial confining pressure and lateral ground movement started. The displacement attained the ultimate state at around 5 second after which the ground was stationary, although the pore water pressure was still high.

Photo 1 reveals the configuration of ground after the ultimate stage. The large displacement was induced by a significant shear distortion of sand. It is important that no slip plane developed. Secondly, the ground surface became level after flow. Since the stability was obtained with a level surface, it is likely that liquefied sand behaved like liquid that has no shear resistance. See the stress-strain behavior of very loose sand (e=0.949) in Fig.1.

The record of excess pore water pressure indicates a slow dissipation. This, however, is not totally due to seepage and consolidation of sand. The lateral movement of ground reduces the overburden pressure above the piezometer, leading to the decrease of total stress. Hence, pore water pressure drops

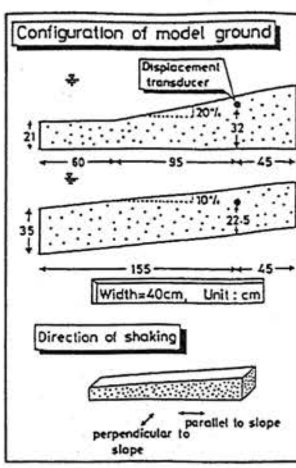

Fig.2 Configuration of model ground.

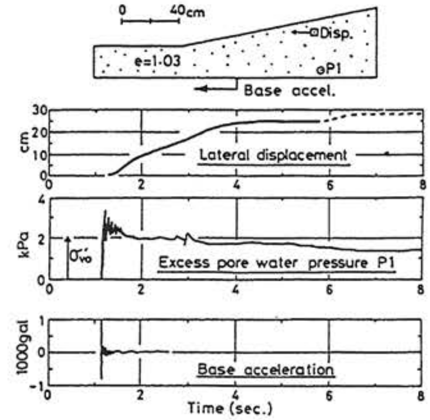

Fig.3 Results of impact test (e=1.03).

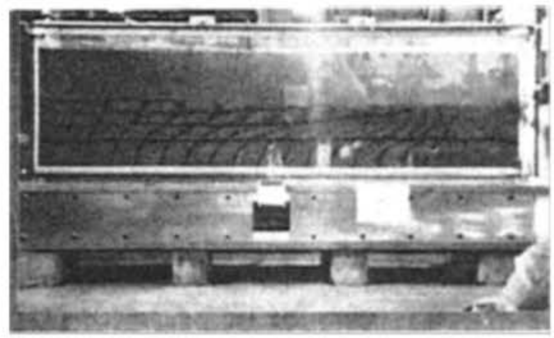

Photo 1 Very loose deposit after flow (e=1.03).

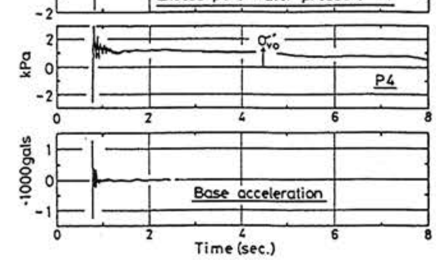

Fig.4 Results of impact test (e=0.95).

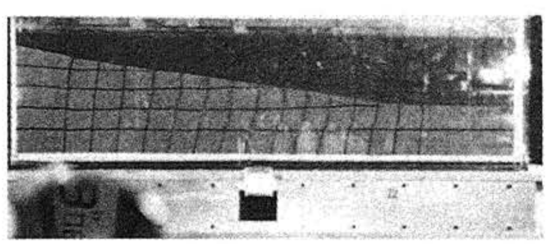

Photo 2 Model ground after flow with e=0.95.

even under undrained conditions.

Fig.4 demonstrates the results of a similar test with void ratio equal to 0.95. Similar to Fig.3, the ultimate displacement was achieved at around 5 second. The effect of increased density was detected in the surface slope after movement (Photo 2). The surface did not became level, suggesting that the sand had a residual strength at large strain that could sustain shear stress in the slope. The recorded reduction of excess pore water pressure with time is mostly due to the loss of overburden.

Similar tests were repeated on the same configuration of model ground with a range of void ratio. The summary in Fig.5 demonstrates that the greater ultimate displacement was associated with the looser density of sand. It is interesting further that the time elapsed in the course of flow was constant, independent of sand density.

Fig.6 illustrates the time history of acceleration of lateral ground movement, This was obtained by taking the second time derivative of the displacement history in Fig.5. The positive acceleration after 1 second shows the initiation of flow, after which the acceleration was negative till the end; the velocity continued to decrease.

Fig.7 shows the displacement time history obtained from 10%-slope tests. When compared with Fig.5, Fig.6 shows that the magnitude of displacement was much smaller when slope was reduced.

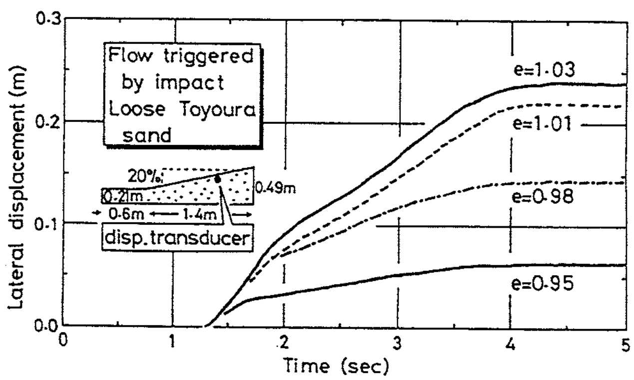

Fig.5 Effects of density on lateral flow.

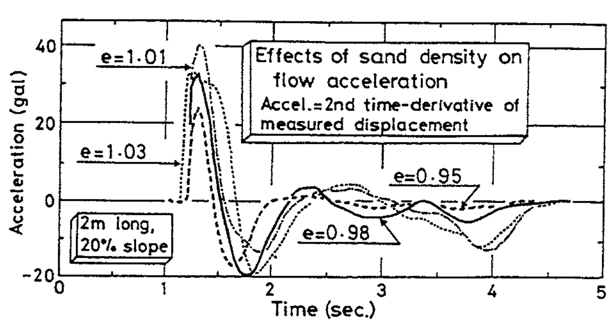

Fig.6 Acceleration of lateral movement.

SOIL FLOW INDUCED BY CYCLIC SHAKING

Model ground of 20% slope was cyclically shaken parallel to the slope (Fig.8). Since the shaking continued for a sufficiently long time, the lateral movement of soil continued for more than 10 seconds. This duration time is longer than what occurred in impulse tests (Fig.5). The magnitude of displacement at e=0.93 is also larger than the that in impulse test at similar sand density (Fig.4). See that the ground surface after flow became level (Photo 3). Thus, a ground subjected to shaking behaves similar to liquid without shear strength, whereas it develops some strength under impulse excitation.

Fig.9 compares the results of impulse (Fig.3) and cyclic shaking tests. Since the sand was very loose, both types of shaking produced a similar extent of ground movement. Duration time of soil flow is similar as well. The level ground surface that was finally attained suggests that shear strength is negligible.

Fig.10 compares the final displacement at the end of flow. The impulse shaking indicates that the final displacement depends on density. When slightly denser, sand is able to flow only a limited distance, while it can move 30 cm after a long duration of cyclic loading. It seems that lateral movement has to stop at the end of limited duration of shaking if the induced displacement is already greater than what can occur under static gravity.

THEORY OF FLOW ANALYSIS

Sasaki et al. (1992) carried out shaking table tests to show that the lateral displacement in liquefied sand, U(x,z), exhibits a sinusoidal distribution in the vertical direction (Fig.11).

$$U(x,z) = F(x) \times (\textit{sin function of } z) \qquad (1)$$

The displacement of soil develops with time from zero to the ultimate value of U after a sufficiently long time of shaking. Since the prediction of U is already possible (Towhata et al., 1992), the present study attempts to calculate the temporal development of displacement, u(x,z,t), from zero to U.

The effects of time is separated from x and z terms (Fig.11);

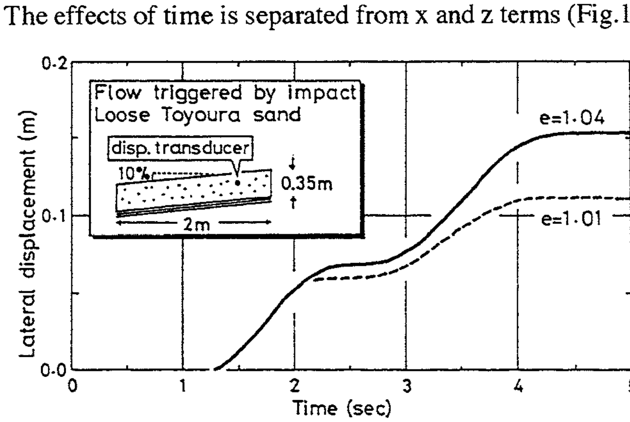

Fig.7 Lateral flow in 10% slope.

$$u(x,z,t) = U(x,z)\lambda(t) \quad (2)$$

By assuming constant-volume (undrained) deformation and substituting Eq.1 in the equation of volume conservation, the vertical displacement, v(x,z,t), is derived in terms of U and λ;

$$\frac{\partial u}{\partial x} + \frac{\partial v}{\partial z} = 0 \quad (3)$$

Moreover, both shear strain ($\partial u/\partial z$) and velocity ($\partial u/\partial t$ and $\partial v/\partial t$) are described in terms of unknown λ at any location and time. Hence, it is possible to calculate the potential energy (Q), due to gravity and strain, as well as the kinetic energy (K) of the ground.

$$K = \int \frac{\rho}{2} velocity^2 dv = \int \frac{\rho}{2} U^2 dv \left(\frac{d\lambda}{dt}\right)^2 \equiv \frac{m}{2}\left(\frac{d\lambda}{dt}\right)^2 \quad (4)$$

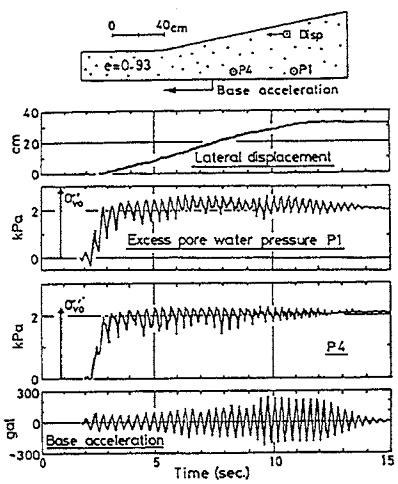

Fig.8 Results of test with cyclic shaking (e=0.93).

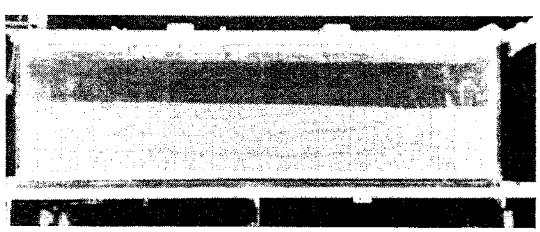

Photo 3 Model ground after cyclic shaking (e=0.93).

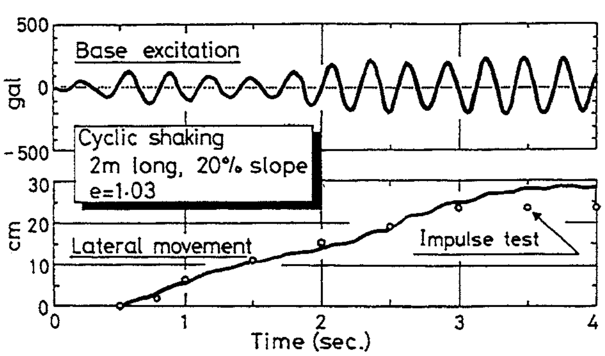

Fig.9 Cyclic shaking compared with impulse test (e=1.03).

in which ρ is the mass density of soil and m is a parameter depending on density and U. Similarly,

$$Q = \frac{k}{2}\lambda^2 + f\lambda \quad (5)$$

where parameters k and f include contributions from gravity, strain, and residual strength of soil, τ_{res}.

An equation of motion in terms of λ is derived by using the Lagrangean equation of motion;

$$\frac{d}{dt}\frac{\partial(K-Q)}{\partial\left(\frac{d\lambda}{dt}\right)} - \frac{\partial(K-Q)}{\partial\lambda} = 0 \quad (6)$$

By substituting Eqs.4 and 5 here;

$$m\frac{d^2\lambda}{dt^2} + c\frac{d\lambda}{dt} + k\lambda = k - r\tau_{res} - n\frac{d^2U_b}{dt^2} \quad (7)$$

wherein $r\tau_{res}$ is of frictional nature and d^2U_b/dt^2 stands for the base acceleration. Eq.7 is solved to obtain a time history of λ, which is then substituted in Eq.2 to calculate the time history of ground displacement.

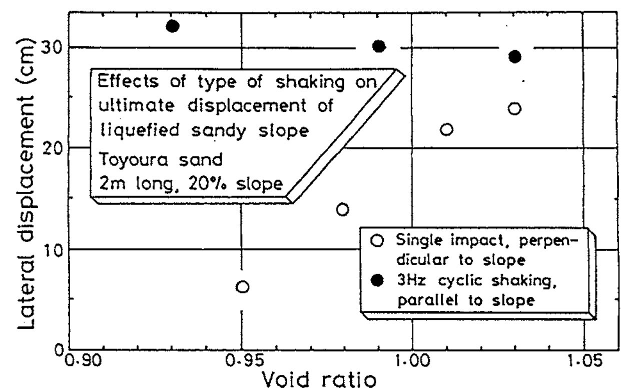

Fig.10 Lateral displacement plotted against void ratio.

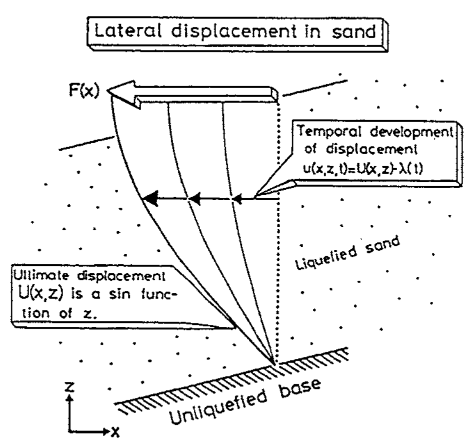

Fig.11 Distribution of lateral displacement along z axis.

RESIDUAL STRENGTH OF LIQUEFIED SAND

The theory described above makes it possible to calculate the displacement at the end of shaking with a variety of residual strength. With the best matching between calculation and observation, conversely, the residual strength was assessed from experimental results. This is summarized in Fig.12. In case of impulse shaking, the strength in the horizontal axis increased as void ratio decreased. On the contrary, the cyclic shaking tests always attained a level surface and the obtained strength is null. Hence, the value of strength employed in calculation should be varied in accordance with the type of shaking; null when cyclic loading is going on, while positive value when flow occurs under static conditions after shaking.

ON VISCOUS TERM

Eq.7 includes a viscous term. Since liquefied sand does not appear to be a viscous material, some discussion is necessary. The velocity-dependent nature of loose liquefied sand was studied by carrying out another model test (Vargas, 1994).

Very loose deposit of Toyoura sand was prepared in a soil container in the same manner as described before. After saturation, a model pipe embedded horizontally in the ground was pulled laterally and the drag force needed for this was monitored. Fig.13 shows that the needed drag force increases

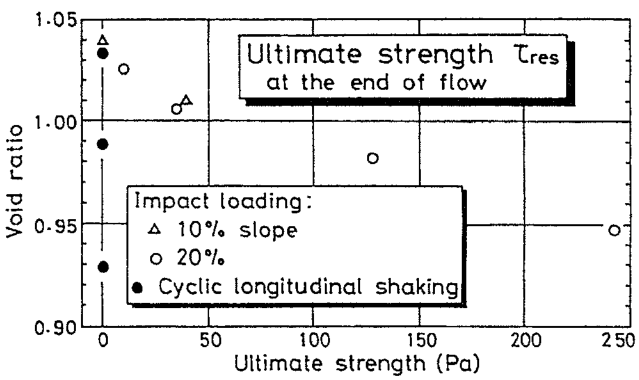

Fig.12 Residual strength of liquefied sand.

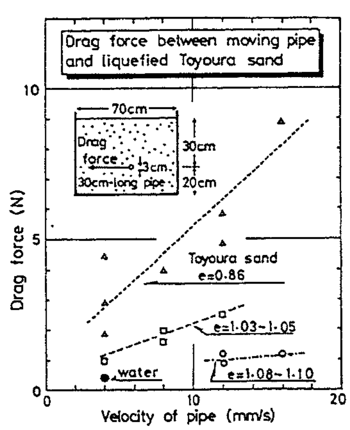

Fig.13 Velocity-dependent nature of liquefied sand.

as sand density increases. More important is that the drag force increases linearly in proportion to the pipe velocity. Although sand grains and pore water do not have a viscous nature very much, their mixture develops a velocity-dependent behavior. Thus, a viscous term in Eq.7 is reasonable.

CALCULATED TIME HISTORY OF DISPLACEMENT

The time history of displacement was calculated by using the theory developed above. The residual strength of sand was determined by using Fig.12, while the viscosity coefficient "c" was determined so that the critical damping ratio (h) in Eq.7 was equal to 0.62.

The cases presented in Fig.5 were analyzed in Fig.14. Subjected to static conditions after impulse, the looser ground attained the greater displacement, whilst the time needed for flow was independent of the density. Thus, the calculation appears to be reasonable. Fig.15 is a similar prediction on 10%-slope models. The calculation is similar to observation in Fig.17.

Fig.16 indicates an analysis on a ground movement under cyclic shaking (Fig.9). The flow occurred quickly as observed experimentally.

The 1983 Nihonkai-chubu earthquake induced liquefaction and a significant lateral soil movement in Maeyama area in Noshiro City. A previous study (Towhata et al., 1992) tried to calculate the displacement in this area. However, it was able to predict only the ultimate displacement, U, that would

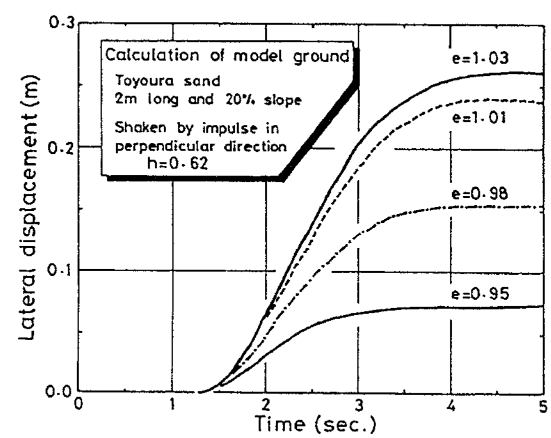

Fig.14 Analysis on 20%-slope model shaken by impulse.

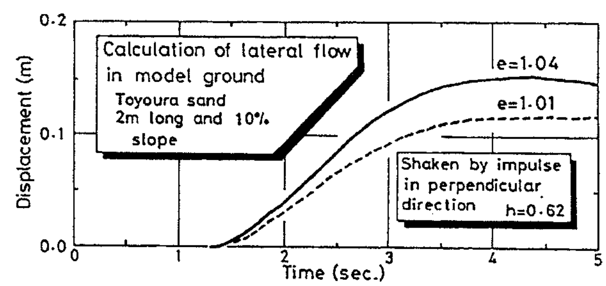

Fig.15 Analysis on 10%-slope model shaken by impulse.

occur if the state of flow continued for a sufficiently long time. Consequently, the prediction overestimated the displacement measured by Hamada et al. (1986).

Fig.17 illustrates the results of new theory in which the time history is taken into account. Since the base motion in this particular site is unknown, a harmonic motion with 150gals in amplitude and 2Hz in frequency were repeated 20 times after onset of liquefaction. This motion seems to be equivalent to the real one. The calculation indicates that λ developed up to 0.77 at the end of shaking. This value gives the distribution of ground displacement which is more or less similar to observation (Fig.17). A minor overestimation that still remains in the calculation is due to the number of cycles which in reality may hot have been so large as 20.

CONCLUSION

A series of shaking-table tests were conducted to study the lateral displacement of liquefied ground. A similarity in stress-strain behavior of sand under large distortion was achieved between reality and small model by employing a very loose density of sand in the laboratory. The test results indicated that the residual strength is null when very loose sand flows under static conditions or even denser sand flows under the effects of cyclic shaking. Otherwise, the strength under static conditions increases with the density of sand. Another tests on pipe movement indicated that there is a viscous nature in liquefied sand. These findings were combined with the theory of ground movement based on the Lagrangean equation of motion. Thus, it became possible to predict the time history of ground flow. The calculation was compared with observation and a good agreement was obtained.

ACKNOWLEDGMENT

The present testing was conducted with Dr. R.P.Orense, Mr. S.Imamura and Mr. K.Kudo. Authors express their gratitude to those contributions.

LIST OF REFERENCES

Hamada,M. et al. (1986) "Observation of Permanent Ground Displacement Induced by Soil Liquefaction," Proc. JSCE, 376/III-6, 211-220.

Horii,K. (1968) chapter on "*Highway Bridges*, "General Report on the Niigata Earthquake, Tokyo Electr. Engg. Coll. Press, 444.

Sasaki,Y. et al. (1992) "Mechanism of Permanent Displacement of Ground Caused by Seismic Liquefaction," Soil Found. (32), 3, 79-96.

Seed,H.B. et al. (1975) "The Slides in the Lower San Fernando Dams during the Earthquake of February 9, 1971," Proc. ASCE, (101), GT7, 651-688.

Taboada,V.M. and Dobry,R. (1993) "Experimental Results of Model No.2," Proc. VELACS Symp., Balkema, 277-294.

Towhata,I. et al. (1992) "Prediction of Permanent Displacement of Liquefied Ground by Means of Minimum Energy Principle," Soil Found. (32), 3, 97-116.

Vargas,W. (1994) "Study on Flowing Liquefied Ground by Means of Model Pipe Tests," Master Thesis, Univ. Tokyo.

Verdugo,R. (1992) "Characterization of Sandy Soil Behavior under Large Deformation," Ph.D.Thesis, Univ. Tokyo.

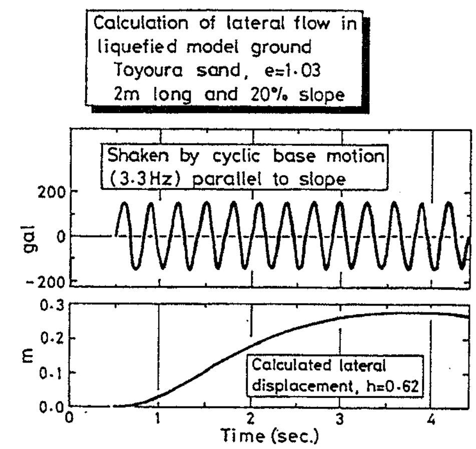

Fig.16 Analysis on 20%-slope model shaken cyclically.

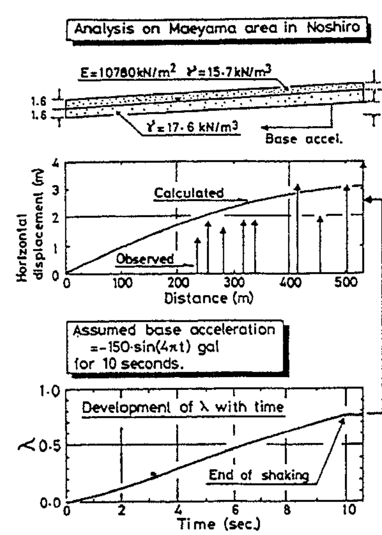

Fig.17 Case study on Noshiro-city slope.